Available online at www.sciencedirect.com
ScienceDirect
Vibrational Spectroscopy 42 (2006) 249–253
VIBRATIONAL SPECTROSCOPY
www.elsevier.com/locate/vibspec

Chalcogenide waveguide structures as substrates and guiding layers for evanescent wave Raman spectroscopy of bacteriorhodopsin

A. Pope [a,b], A. Schulte [a,b,*], Y. Guo [a,b], L.K. Ono [a], B. Roldan Cuenya [a], C. Lopez [b], K. Richardson [b,c], K. Kitanovski [a], T. Winningham [a]

[a] Department of Physics, University of Central Florida, 4000 Central Florida Blvd., Orlando, FL 32816, USA
[b] College of Optics and Photonics-CREOL, University of Central Florida, 4000 Central Florida Blvd., Orlando, FL 32816, USA
[c] School of Materials Science and Engineering, Clemson University, Clemson, SC 29634, USA

Available online 19 June 2006

Abstract

We investigate composite structures where a chalcogenide waveguide provides the substrate and the guiding layer for a bacteriorhodopsin film whose Raman spectrum is desired. Plasma exposure of the chalcogenide substrate allows for a hydrophilic surface to which organic layers can easily adhere. Surface morphology, structure, and chemical composition are characterized by X-ray photoelectron spectroscopy. A 785 nm beam from a Ti:Sapphire laser was coupled into the As_2S_3 waveguide and the evanescent field was employed to excite Raman scattering in the bacteriorhodopsin film. The Raman spectrum of the bacteriorhodopsin film in the fingerprint region is indicative of the native conformation and it shows that the protein is in the light adapted state.

Keywords: Raman spectroscopy; Chalcogenide glass waveguides; Bacteriorhodopsin

1. Introduction

Chalcogenide glasses (ChGs) have shown promise in integrated optics applications due to their high transmission at optical communication wavelengths and the capability to create integrated components with one- and two-photon laser writing [1,2]. In the microstructural analysis of thin film devices, Raman spectroscopy employing integrated optical techniques provides a non-destructive probe with good molecular specificity and high sensitivity [3–5]. Previously, we have applied waveguide Raman spectroscopy (WRS) using guided mode excitation to chalcogenide glasses to obtain *in situ* structural information of the waveguide itself [6,7]. Here we investigate composite structures where a chalcogenide waveguide provides the substrate and the guiding layer for a biomolecular film whose Raman spectrum is desired.

Optical components based on As_2S_3 glasses have been widely used for infrared optical applications since the glasses' initial development. For the integration of waveguide structures with photo-sensitive proteins bacteriorhodopsin (bR) is of particular interest, since there are applications in molecular electronic devices and optical switching that are of considerable interest [8–11]. The primary function of bR is as a photon driven proton pump in halobacterium halobium, thus converting light energy into chemical energy. Photon absorption is followed by charge transport and significant shifts of the electronic absorption spectra while undergoing a photo-chemical cycle [12,13].

In this contribution we show that evanescent waves can provide localized optical probes for thin layers of bacteriorhodopsin. Arsenic trisulfide (As_2S_3) waveguides are processed and characterized to allow for the homogeneous deposition of bR film layers. We demonstrate that evanescently excited near-infrared Raman spectra can be measured with high signal-to-noise ratio providing an *in situ* probe of the native state of the protein.

2. Experimental

The waveguide structure consists of an As_2S_3 ChG film on a SiO_2 substrate with channels grooved into the glass surface to allow for light wave propagation. Single layer waveguides were

* Corresponding author. Fax: +1 407 823 5112.
E-mail address: afs@physics.ucf.edu (A. Schulte).

0924-2031/$ – see front matter © 2006 Elsevier B.V. All rights reserved.
doi:10.1016/j.vibspec.2006.05.006

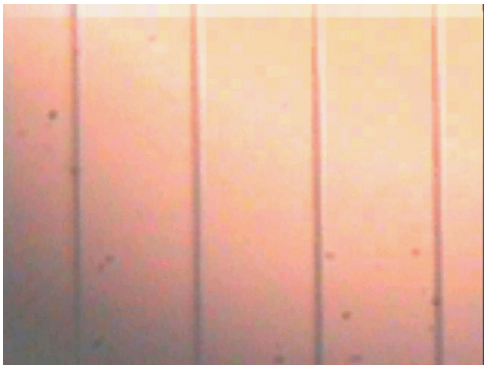

Fig. 1. Optical image of As_2S_3 lithography etched channels.

deposited via thermal evaporation of As_2S_3 bulk glasses on silicon substrates as previously described [14]. Fig. 1 shows a top view of the lithography etched channels in the As_2S_3 film. Waveguides are 1.5–2.5 μm thick. The etched grooves were measured by an atomic force microscope to be approximately 0.15 μm high with a width varying from 1 to 10 μm.

It is believed that the originally hydrophobic ChG film becomes hydrophilic after exposure to O_2 plasma due to oxygen adsorption and/or chemisorption at the surface of the film. This in turn allows for hydrogen bonding with an aqueous protein solution. To explore this hypothesis, XPS was employed. The As_2S_3 films were exposed to O_2 plasma at a pressure of 2×10^{-2} Torr for approximately one minute. Three 100 μL portions of aqueous bR solution were deposited with a micropipette on the As_2S_3 film and allowed to dry under vacuum. Two films were measured, one of them "as-deposited", the other after having been exposed to O_2 plasma for five minutes immediately before measurements. The pre- and post-treatment surface chemistry of the waveguide samples was studied using a SPECS Phoibos 100 mm electron spectrometer operated at a vacuum of $\sim 2 \times 10^{-10}$ mbar. A non-monochromatic Al X-ray source at a power of 245 W and pass energy of 50 eV was used for analysis. Irradiation occurred at an angle of approximately 30° to the surface of the films.

The binding energy (BE) scale displayed in Fig. 2 has been calibrated using the adventitious C 1s XPS peak at 284.6 eV [15,16]. BE shifts of +2.0 and +2.6 eV were measured before and after O_2-plasma exposure due to charging of the insulating glass support.

The Raman spectroscopy experimental setup uses a 785 nm output beam from a continuous mode Ti:Sapphire (Schwarz Electro-Optics) laser with 25 mW power coupled into a As_2S_3 waveguide via a 20× microscope objective. Propagation was verified by observing the mode at the waveguide output. The

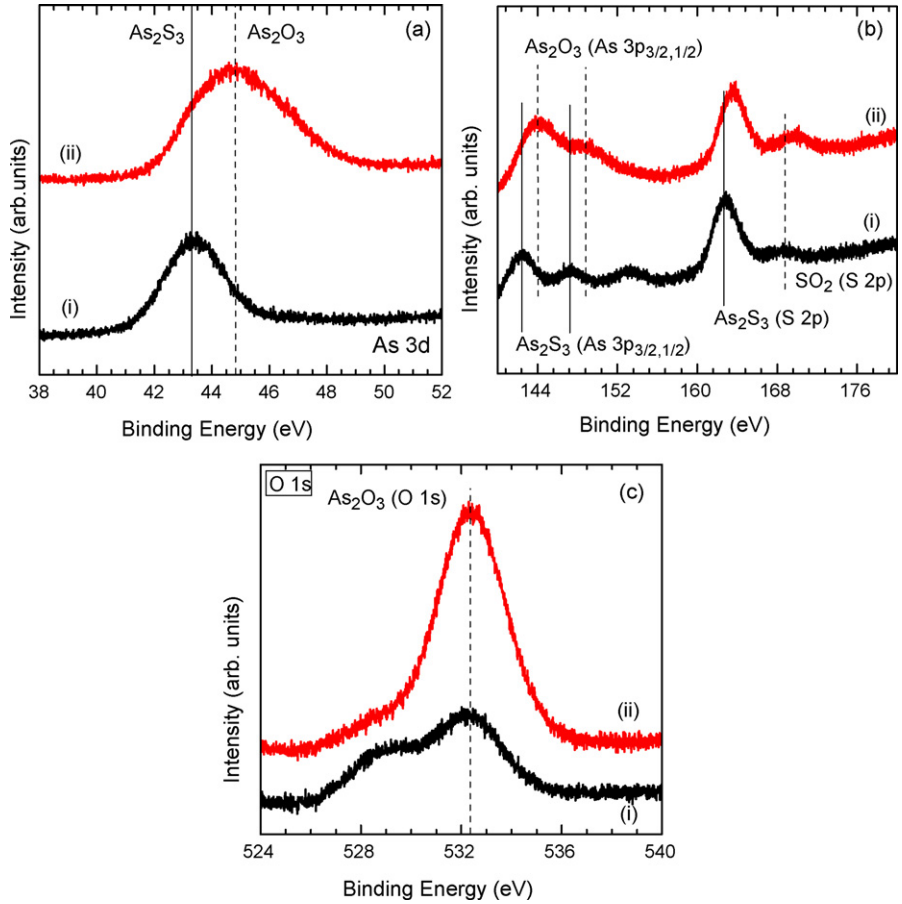

Fig. 2. XPS spectra of a As_2S_3 waveguide measured before (i) and after (ii) O_2 plasma exposure. The spectral bands of As 3d electrons are shown in (a), As 3p and S 2p in (b) and O 1s in (c).

90° Raman scattered light emanating from the top surface of the film under examination was collected with a lens and spectrally analyzed with a back-illuminated, thinned CCD detector (Princeton Instruments) mounted on the exit port of a single grating spectrograph (HR 640, JY Horiba). The Rayleigh line was suppressed by a CdTe bandgap filter.

3. Results and discussion

The first step to using evanescent wave excitation of a protein layer is to ensure the adhesion of a thin aqueous bR layer to the glass. The direct exposure of the As_2S_3 ChG film to O_2 plasma made its surface hydrophilic.

The XPS spectra corresponding to plasma exposed As_2S_3 film (top curve) and a non-exposed As_2S_3 film (bottom) are shown in Fig. 2. Before plasma treatment (Fig. 2(a(i))), a spectral line is observed at 43.4 eV. This line has previously been attributed to the 3d orbital of As bound to S in the As_2S_3 structure [17,18]. After taking into consideration the corresponding atomic sensitivity factors and appropriate background subtraction [19,20], the analysis of the relative intensities of the S and As XPS peaks (Fig. 2(b)) confirmed As_2S_3 as main component of our As_xS_y waveguides. This spectral line becomes broader after O_2 plasma exposure (Fig. 2(a(ii))) and is shifted +1.5 eV due to the contribution of As–O bonding (44.8 eV peak).

The position of the XPS peak associated to the As 3p orbital (144 eV, Fig. 2(b(ii))) also confirms the formation of As_2O_3 after O_2 plasma exposure, with a BE shift of +1.6 eV with respect to As 3p in As_2S_3. The spectral lines at 162.7 and 168.8 eV in Fig. 2(b(i)) can be assigned to S 2p in As_2S_3 and SO_2 [15], respectively. After plasma exposure, both lines appear shifted by 1 eV. In Fig. 2(b), a XPS peak at 153.4 eV initially attributed to a surface impurity disappeared after the plasma treatment.

A stronger oxygen signal is observed at approximately 532.3 eV on the As_2S_3 film after O_2 plasma exposure, Fig. 2(c(ii)). This BE is associated to O 1s in As_2O_3. Our XPS data also show the removal of further surface impurities (i.e. 528.9 eV peak) upon plasma exposure. No contribution of the underlying SiO_2/Si support was observed by XPS due to the thickness of the As_2S_3 film (1.5–2.5 μm).

The mode profile of the As_2S_3 film was investigated by approximating the waveguide structure to be a slab waveguide. This approximation was deemed valid due to the small channel depth in comparison with the overall film. The analysis of optical wave transmission in a dielectric slab waveguide follows from Maxwell's equations. Following Ref. [3] the electric field distribution for a planar geometry was calculated. For this a program using LabVIEW™ software was created [21]. For each mode propagating through the ChG guiding layer there is an effective refractive index, n_{eff}, in the range between that of the ChG and SiO_2 glass substrate. If the index of the adsorbed layer, n_c is higher than n_{eff} of a specific mode, the mode will be guiding in both layers. If n_c is less than n_{eff}, the wave is evanescent in the adsorbed layer [5]. The refractive index of SiO_2 is ~1.45 and the refractive index of As_2S_3 is

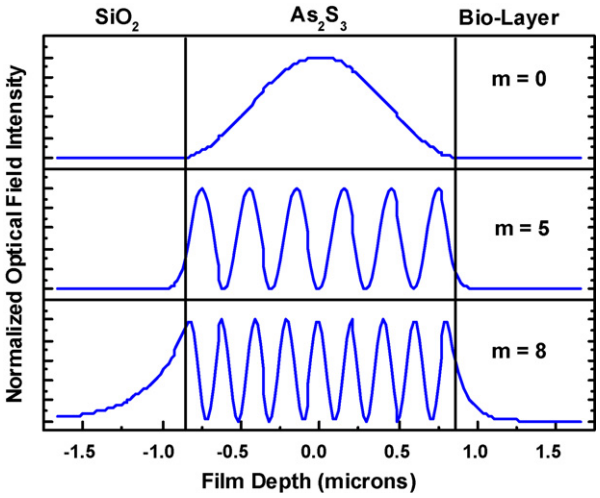

Fig. 3. Optical field intensity for modes number $m = 0$, 5, 8 (see text) as a function of film depth for 1.66 μm thick As_2S_3 film on SiO_2 substrate with biological assembly of $n = 1.33$ cladding at 785 nm excitation wavelength.

~2.45 using the 785 nm wavelength excitation radiation; therefore, $1.45 < n_{eff} < 2.45$ for the As_2S_3 ChG film. For proteins, the refractive index can be assessed to be that of water; therefore, $n_c \sim 1.33$. Since n_c is less than the minimal value of n_{eff}, it is the evanescent tail of the guided wave that is responsible for the Raman spectrum. The refractive indices used for the model were 1.33, 2.45, and 1.45 for bR, As_2S_3 and SiO_2, respectively. Due to the high refractive index of the ChG film there are many propagation modes. It was determined that the As_2S_3 film has nine ($m = 0$–8) modes. Fig. 3 shows the optical field intensity of three modes ($m = 0$, 5, 8) for the experimental geometry. Mode eight is the one most evanescent into the biolayer. To elucidate the difference in the fraction of radiation power guided in the biolayer for the various modes, the areas of the evanescent electric field intensity of modes $m = 0$–8 were determined by integration. The radiant power coupled into the protein layer at a wavelength of 785 nm is highest for mode $m = 8$. Normalized to this mode the area ratios of modes $m = 0$–7 are 0.002, 0.01, 0.023, 0.045, 0.079, 0.14, 0.23, and 0.43, respectively.

Fig. 4 displays an SEM picture of a 1.5 μm thin film of bR on a ChG waveguide whose Raman signal was measured. There are no restrictions on the thickness of the bR film [22]. The

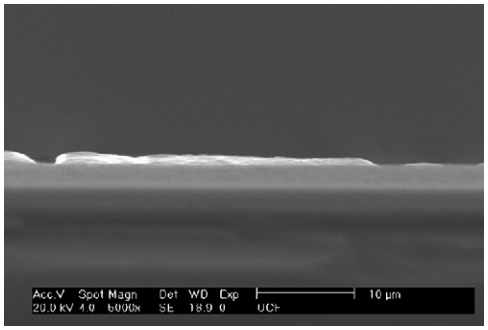

Fig. 4. SEM image of 1.5 μm bacteriorhodopsin layer on ChG waveguide. The scalebar corresponds to 10 μm.

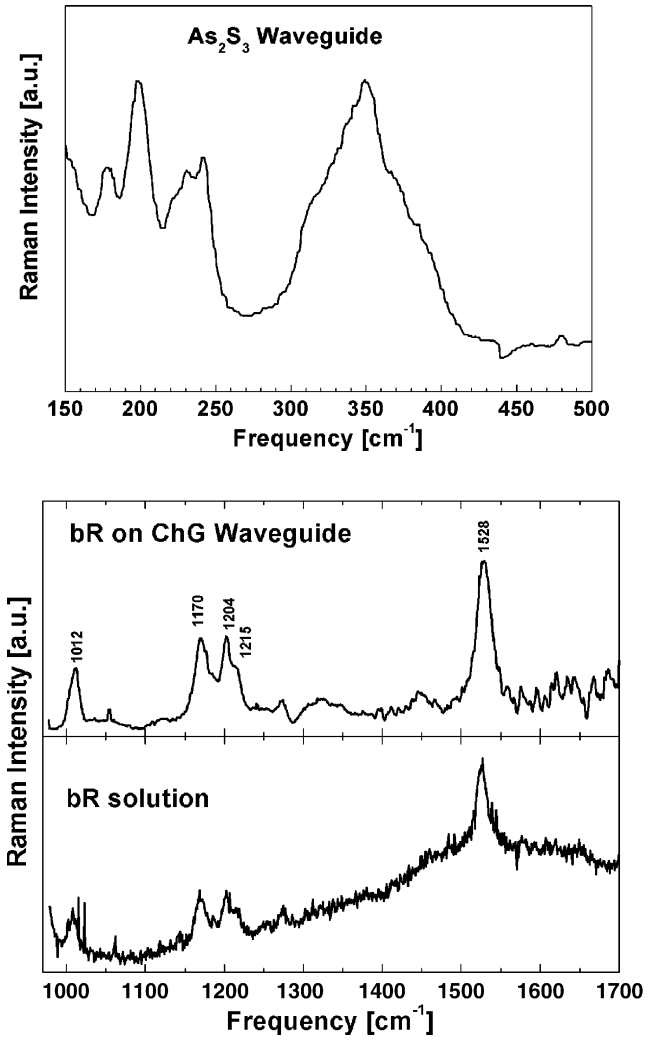

Fig. 5. (a) Raman spectrum of a As_2S_3 ChG waveguide measured with guided mode excitation. (b) Evanescent wave excited Raman spectrum of a bacteriorhodopsin layer on a ChG waveguide and of bacteriorhodopsin in aqueous solution. The laser excitation wavelength is 785 nm.

Raman spectrum of the As_2S_3 waveguide is shown in Fig. 5(a). The Raman active vibrations have frequencies less than 500 cm^{-1}. The dominant band between 300 and 400 cm^{-1} is attributed to AsS_3 pyramidal units and their interactions, while vibrations due to S–S bonds are observed below 300 cm^{-1} [17]. Fig. 5(b) displays the Raman spectra obtained from bR layered on the waveguide substrate and from bacteriorhodopsin in aqueous solution. Both spectra show the same features, though a slight fluorescence background is visible in the solution spectrum. As with all proteins and organic assemblies, the characteristic vibrational frequencies of bR are in the 1000–4000 cm^{-1} range. Thus no interference of substrate vibrations with the signal from the protein is minimized. The bR spectra in Fig. 5(b) are indicative of the light adapted state [22]. The light adapted form of bR is the initial state for the proton pumping cycle. At an excitation wavelength of 785 nm the Raman spectrum is still associated with the vibrations of the atoms that comprise the chromophore. Resonance Raman, nuclear magnetic resonance (NMR), and chemical extraction studies have established that the chromophore in light adapted bR is a $C_{13} = C_{14}$ trans, $C_{15} = NHR$ trans protonated Schiff base of retinal [22]. As shown in Fig. 5(b), bR has several vibrational frequencies that are identifiable. The band at 1012 cm^{-1} is assigned to the rocking vibrations of a C–CH_3 group of the bR molecule. The 1100–1300 cm^{-1} region of the Raman spectrum is the fingerprint region for C–C bonds and is very sensitive to isomerization. The intense band at 1528 cm^{-1} is attributed to the ethylenic stretching mode of C=C bonds [22].

4. Conclusions

We have demonstrated that evanescent wave excited Raman spectra with high signal-to-noise ratio can be measured on a bacteriorhodopsin film deposited from aqueous solution on a chalcogenide glass waveguide. The Raman spectrum of the bR layer excited at 785 nm shows that the protein is in the light adapted state. The use of ChG films is beneficial due to their Raman signal in the low frequency range not interfering with the fingerprint region of the protein. The low vibrational frequencies of the As_2S_3 waveguide makes the film a viable substrate for biological assemblies in general. The use of XPS to characterize the O_2 plasma exposed film and the "as deposited" film proved to be a valuable tool in the surface analysis of the As_2S_3 film. Through analysis of the XPS results it was determined that oxygen will adsorb to the surface of the film creating a hydrophilic surface. Exposure to O_2 plasma proved to be an efficient technique to prepare hydrophilic ChG films allowing for deposition of protein layers from aqueous solution.

ChG waveguides are optimized for near-infrared excitation allowing to obtain the Raman spectra of biological compounds at minimal background fluorescence. This feature of the substrates can be a useful tool in the study of cells and microorganisms. Obtaining the Raman spectra at wavelengths less than 1 μm allows for the resolution of small spatial features compared to mid-infrared absorption wavelengths of 5–10 μm. Integrated optical components fabricated with ChG can be combined with proteins such as bR. Evanescent wave excitation may be employed for optical switching and spectroscopy of bio-assemblies on patterned ChG semiconductors. There are also possible applications involving bio-molecular sensors.

Acknowledgments

We thank N. Ho, R. Vallee, and L. Chernyak for assistance and advice with chalcogenide waveguides. We are grateful to S. Balashov (UC Irvine) for providing bacteriorhodopsin samples. This work was supported in part by NSF grants DMR-0312081, ECS-0123484, and DMR-0421253.

References

[1] M. Asobe, T. Kanamori, K. Kubodera, IEEE J. Quantum Electron. 29 (1993) 2325.
[2] A. Zoubir, M. Richardson, C. Rivero, A. Schulte, K. Richardson, N. Ho, R. Vallee, Opt. Lett. 29 (2004) 748.

[3] J.F. Rabolt, in: J.F. Rabolt, D.B. Chase (Eds.), Fourier Transform Raman Spectroscopy from Concept to Experiment, Academic Press Inc., San Diego, CA, 1994 , pp. 133–156 (Chapter 5).
[4] J.F. Rabolt, R. Santo, J.D. Swalen, Appl. Spectrosc. 34 (5) (1980) 517.
[5] J.P. Rabe, J.D. Swalen, J.F. Rabolt, J. Chem. Phys. 86 (3) (1987) 1601.
[6] A. Schulte, C. Rivero, K. Richardson, K. Turcotte, J. Laniel, V. Hamel, A. Villeneuve, A. Saliminia, T. Galstian, Opt. Commun. 198 (2001) 125.
[7] A. Schulte, K. Richardson, Recent Res. Dev. Non-Cryst. Solids 2 (2002) 143.
[8] P. Ormos, L. Fábián, L. Oroszi, E.K. Wolff, J.J. Ramsden, A. Dér, Appl. Phys. Lett. 80 (20) (2002) 4060.
[9] C.P. Singh, S. Roy, Opt. Commun. 218 (2003) 55.
[10] S. Roy, P. Sharma, A.K. Dharmadhikari, D. Mathur, Opt. Commun. 237 (2004) 251.
[11] L. Fabian, L. Orosozi, P. Ormos, A. Der, NATO Sci. Series II: Math. Phys. Chem. 96 (2003) 341.
[12] K.J. Wise, N.B. Gillespie, J.A. Stuart, M.P. Krebs, R.R. Birge, Trends Biotechnol. 20 (9) (2002) 387.
[13] N. Hampp, Chem. Rev. 100 (5) (2000) 1755.
[14] C. Lopez, K.A. Richardson, S. Seal, D.K. Verma, A. Graham, A. Villeneuve, T.V. Gastian, K. Turcotte, A. Saliminia, J. Laniel, M. deCastro, A. Schulte, C. Rivero, Am. Ceram. Soc. 85 (2002) 1372.
[15] National Institute of Science and Technology (NIST) XPS Database (http://srdata.nist.gov/xps/).
[16] J.F. Moulder, W.F. Stickle, P.E. Sobol, K.D. Bomben, in: J. Chastain, R.C. King, Jr. (Eds.), Handbook of X-ray Photoelectron Spectroscopy, Physical Electronics Inc., MN, 1995.
[17] W. Li, S. Seal, C. Rivero, C. Lopez, K.A. Richardson, A. Pope, A. Schulte, S. Mynemi, H. Jain, K. Antoine, A. Miller, J. Appl. Phys. 98 (2005) 053503.
[18] S. Seal, K.A. Richardson, C. Lopez, A. Graham, D.K. Verma, Phys. Chem. Glasses 43 (2002) 59.
[19] D. Briggs, M.P. Seah (Eds.), Practical Surface Analysis. Auger and X-ray Photoelectron Spectroscopy, vol. 1, John Wiley and Sons, Chichester, UK, 1990.
[20] D.A. Shirley, Phys. Rev. B 5 (1972) 4709.
[21] A. Pope, B.S. Honors Thesis, University of Central Florida, Orlando, FL, 2005.
[22] R.A. Mathies, S.O. Smith, I. Palings, in: T.G. Spiro (Ed.), Biological Applications of Raman Spectroscopy, vol. 2, Wiley, New York, 1987 , pp. 59–108 (Chapter 2).